Electrical and tribological behaviour of gold/gold sliding contacts of the wire/ring type for slip ring applications

Corentin Ferreira, Aurore Brézard-Oudot, Manon Isard, Sophie Noël, Frédéric Houzé, Philippe Teste

▶ **To cite this version:**

Corentin Ferreira, Aurore Brézard-Oudot, Manon Isard, Sophie Noël, Frédéric Houzé, et al.. Electrical and tribological behaviour of gold/gold sliding contacts of the wire/ring type for slip ring applications. 68th Holm Conference on Electrical Contacts, Oct 2023, Seattle (USA), Washington, United States. pp.278-284, 10.1109/HOLM56075.2023.10352303 . hal-04207904

HAL Id: hal-04207904

https://centralesupelec.hal.science/hal-04207904

Submitted on 14 Sep 2023

HAL is a multi-disciplinary open access archive for the deposit and dissemination of scientific research documents, whether they are published or not. The documents may come from teaching and research institutions in France or abroad, or from public or private research centers.

L'archive ouverte pluridisciplinaire **HAL**, est destinée au dépôt et à la diffusion de documents scientifiques de niveau recherche, publiés ou non, émanant des établissements d'enseignement et de recherche français ou étrangers, des laboratoires publics ou privés.

Electrical and tribological behaviour of gold/gold sliding contacts of the wire/ring type for slip ring applications

Corentin Ferreira[1,2], Aurore Brézard-Oudot[1], Manon Isard[2], Sophie Noël[1], Frédéric Houzé[1]; Philippe Testé[1]

[1] Université Paris-Saclay, CentraleSupélec, CNRS, Laboratoire de Génie Électrique et Électronique de Paris, 91192, Gif-sur-Yvette, France, Sorbonne Université, CNRS, Laboratoire de Génie Électrique et Électronique de Paris, 75250, Paris, France
[2] Everaxis Aerospace & Defence, 92350, Le Plessis-Robinson, France

Abstract— **Many industrial systems require the transmission of electrical current from a static part to a rotating one. This is achieved by a sliding contact within a slip ring device. These devices usually have to be fully operative for many years. Understanding the wear mechanism and the electrical behaviour are of major interest. In order to study the triboelectrical behaviour of sliding contacts of the wire/ring type, a rotating ball-on-disc tribometer (Anton Paar TRB^3) has been used. The friction of a wire on a ring is reproduced by the friction of a wire on a disc thanks to a special wire holder. The gold alloy wire is the same as in the real slip ring device and the brass disc has the same gold alloy plating as in real slip rings. Voltage drop through the interface is measured with the 4-probes method. This set-up allows to study the influence of various parameters such as rotating speed, current value, normal force, lubrication conditions, and more. In this paper, the new experimental setup, and the first results obtained during its implementation are presented.**

Keywords—Slip ring, Gold contact, Electrical sliding contact, Tribometer

I. INTRODUCTION

In order to transmit electrical power and signal between a stationary and a rotary machine part, slip rings are used. To that purpose, various designs can be used as well as various materials depending on the environmental conditions and geometry. Many phenomena are happening on the contact surface during sliding, such as friction, wear, and transfer, which need to be understood for a better comprehension of the system. The flow of current at the contact interface also involves the generation of electrical noise. The electrical noise arises from the variation of the contact voltage related to the number of contact spots between the two elements during friction; a higher number of contact spots implies a larger contact area, which has a lower contact voltage than a small contact area. For this goal, a tribometer test device has been adapted with which the friction properties are measured in parallel to the contact resistance.

The slip ring design presented in this paper is represented in Fig. 1. The electricity flows between structures thanks to a sliding contact composed of a 0.4 mm diameter bulk gold-alloy wire confined in a V-groove geometry of a 40 mm diameter hard gold alloy-plated ring, forming the slip ring system. In this way, the wire is in double contact with the ring and ensures both, the contact resistance as well as the contact force. To improve the durability and reliability of the contact over time, contact zones are multiplied by adding a second wire in the same V-groove facing the first one, and are lubricated with a standard synthetic oil. Such systems are widely used for a large variety of industrial applications such as the de-icing of rotary wings for helicopters, pitch control systems for wind power, bottle filling machines, etc.

In general, the majority of tests for the understanding of tribological and electrical contact phenomena are carried out on model slip rings. In numerous studies [1-3], the understanding of the electrical and mechanical properties within the contact is achieved by monitoring the electrical performance during the test and by observing and analysing the surface conditions after testing. Occasionally, monitoring of the coefficient of friction during the test is also carried out. For this purpose, Holzapfel [4] used a slip ring with an instrumented wire/ring contact. This setup allows to follow the contact resistance, thanks to a 4-probes method, during the test, in parallel with the friction force. Also, Smith [5], as part of a tribological system optimisation, used a cross-rod tribometer to simplify the geometry of the samples in contact, and to access the coefficient of friction and the electrical performance of the system during the test.

Furthermore, much work has been done on metal-to-metal electrical sliding contact without being specific to slip rings. The study of coatings, whether for gold plating [6] or for undercoats [7], and the study of the tribological and electrical behaviour of metals [8] are at the origin of various papers. For the study of contacts between metals, the use of a tribometer is common. This device enables to control the test conditions, and to simplify the geometry of contacts allowing to instrument more easily. This simplification also facilitates the observation and the analysis of the post-test samples. Antler [7-8] has extensively studied contact between metals and especially between noble metals. In his work, he used an instrumented pin-on-plane tribometer to monitor the coefficient of friction and the contact resistance during the test. The normal load applied by the pin is achieved via a dead weight; a stress ring is used to acquire the frictional force resulting from the contact between the fixed pin and the rotating plane. For the electrical part, a slip ring under the rotating plane guarantees the current flow and the electrical measurement.

In this study, a new setup has been developed to reproduce the real contact configuration of slip rings. The friction force is measured in parallel with the contact resistance by using a 4-probes method. The main purpose of the present paper is *(i)* to describe a new experimental setup for the investigation of tribological and electrical properties of wire/ring sliding contacts, *(ii)* to detail the data acquisition method, and *(iii)* to present the first results obtained during the implementation of the experimental setup.

Corresponding author: Corentin FERREIRA; Email: corentin.ferreira@centralesupelec.fr

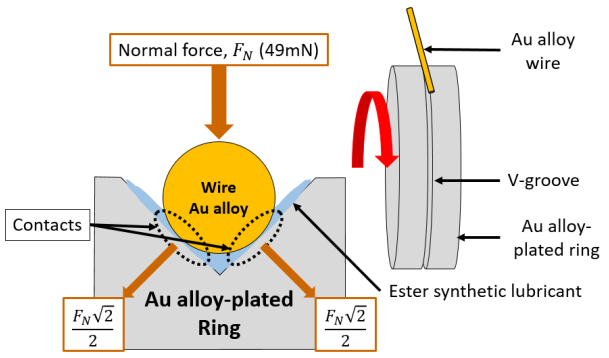

Fig. 1. Illustration of the wire/ring contacts

II. Experimental Setup

To study the tribological and electrical behaviour of the gold-alloy plating of the slip ring system, a tribometer has been used. The TRB^3 tribometer from Anton Paar is initially configured to study the ball/disc contact in pure sliding condition. In this device, the disc is held by a chuck, which rotates at the desired speed. The ball specimen is held stationary in a stainless steel holder, which is attached to the measurement arm as can be seen under n°1 in Fig. 2. The normal force (F_N) applied on the ball via the stainless steel holder is achieved by a dead weight system. Two LVDT sensors allow to collect the tangential force (F_T) by detecting tangential displacements of the arm, and permit to access to the coefficient of friction (μ) through the relation: $\mu = F_T/F_N$. The presence of these two sensors not only improves sensitivity compared to a single sensor, but also eliminates risks of drift due to dimensional variations of the measuring arm with temperature. Technical data of the tribometer are detailed in Table 1.

In order to be representative of the real contact configuration, the tribometer needs to be adapted by modifying the contact configuration and the electrical supply of the contact.

A. Adaptation of the contact configuration

The use of the tribometer allows the study of one of the two contacts in the wire/ring configuration. The contact geometry of this device requires the ring to be represented by a disc (Ø50 mm) of the same substrate, and coated according to an identical protocol as can be seen under n°2 in Fig. 2. The ball is replaced by a curved wire (same as in a real device) mounted in a special holder as shown under n°3 in Fig. 2. The special holder has a groove to fit the wire, and two wedges to constrain it.

In the real case of a wire in contact with the face of a V-groove of a ring, the most representative simplified geometry is that of two cylinders in contact at 90°. In this paper, the wire is a 0.4 mm diameter cylinder and the ring is a 40 mm diameter cylinder. In the real system, the wire applies a normal force of 34.68 mN to the face of a V-groove. According to the Hertz theory, this results in a maximum contact pressure of 0.278 GPa. In the case of a curved wire contact on a flat disc with the tribometer's minimal normal force of 0.25 N, a radius of curvature of more than 1.5 metres is required to achieve the same maximum contact pressure. For this study, it was chosen to transfer the radius of curvature of the real contact ring (20 mm) to the special holder, which results in a higher maximum contact pressure than in the real contact configuration: 0.589 instead of 0.278 GPa.

B. Electrical measurements on the contact

Another important aspect of the real contact is the current supply. In this device, the disc representing the ring is rotating and the wire placed in the special holder is fixed. The use of cables directly connected to the wire is made possible by the design of the special holder as can be seen under n°4 in Fig. 2. On the side of the disc, the operation is more complex because of the rotation. Like the wire rubbing in a V-groove of a ring, the adopted solution is to have a brush made up of a set of wires rubbing with the side of the disc as can be seen under n°5 in Fig. 2. The brush is composed of about ten wires, which makes the contact with the smooth surface of the disc's side more reliable. Moreover, as the measurement arm and the chuck are conductive, it is necessary to insulate the sample holder from the chassis. For this purpose, POM (polyoxymethylene), and glass fibre materials are used, respectively for the wire and for the disc.

Hence, the current flow in the contact provides the opportunity to instrument the system in order to measure the contact resistance during the test. For this purpose, a 4-probes method has been implemented by adding a second connection on each sample holder: a second cable is linked to the wedge of the specific holder for the wire, and a second brush slides against the side of the disc. This is described in Fig. 3 where we can observe a schematic representation of the electrical circuit and the contact voltage measurement system. The electrical supply is guaranteed by a current source, Keithley 2450. As the measured contact voltage is low, it is necessary

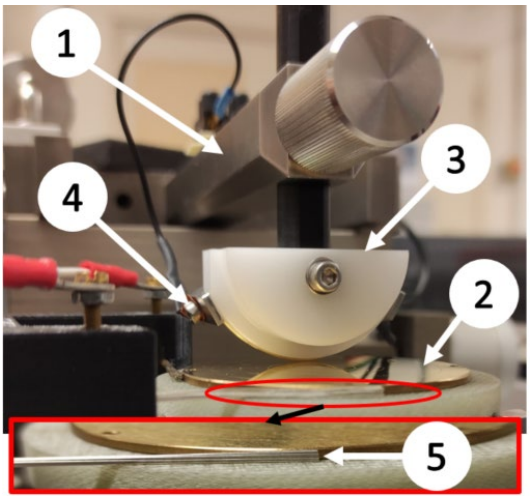

Fig. 2. Picture of the modified TRB^3 tribometer – 1. Measurement arm; 2. Disc; 3. Special holder containing the wire; 4. Cable connected to the wire; 5. Brush sliding against the side of the disc

TABLE I. Technical Data of the Anton Paar TRB^3 Tribometer

Designation	*Units*	*Range*
Rotating speed	RPM	[0.2;2000]
Max linear speed	m/s	5.24
Normal force	N	[0.25;60]
Tangential force	N	up to 5
Tangential force resolution	mN	0.015
Acquisition rate	Hz	[0.01;400]

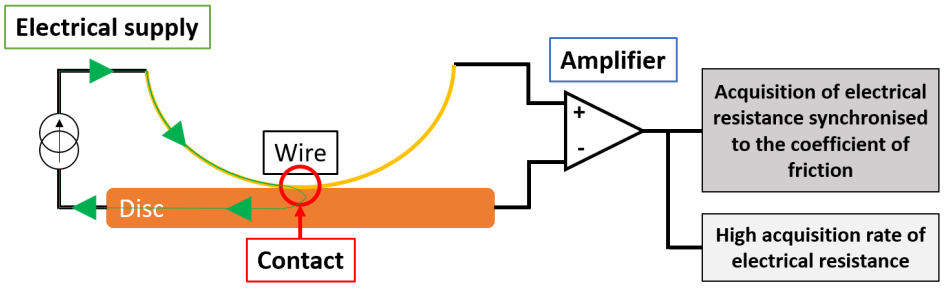

Fig. 3. Electrical diagram of the contact with the 4-probes method

to pass the signal through an amplifier, Stanford Research Systems SR560, before being collected by the acquisition systems.

Then, the acquisition is done on two different devices: the tribometer directly and a fast acquisition system, named Gnostic. The tribometer has the ability to acquire external data through dedicated channels. The advantage of its use is to directly obtain electrical data synchronised with the internal data (friction coefficient, angle, laps, time, etc.). The second device allows the collection of more precise data thanks to a higher acquisition rate: the maximum acquisition frequency is 44 MHz compared to a maximum of 400 Hz for the tribometer. Also, it is possible, thanks to a threshold value, to carry out a fast acquisition over a given period of time at a higher frequency than the initial working frequency. The parallel use of these two devices has the advantage of obtaining a contact voltage measurement synchronised with the evolution of the coefficient of friction, and an acquisition of the contact voltage at a higher frequency to detect possible contact loss.

III. Experimental Methods

The test setup has been described above and the test conditions are summarized in Table 2. No lubricant was used during the tests, unlike the real configuration of slip rings. The different layers that form the coating of the disc are shown in Fig. 4. Note that the gold-alloy plating of the disc is covered by a thin finish layer, which is composed of more gold than the major layer, AuCuX.

The data acquired during the tests are processed using the software MATLAB. With the current intensity, it is possible to calculate the contact resistance thanks to the acquisition of the contact voltage. On the tribometer, synchronised data acquisition allows the coefficient of friction and contact resistance to be extracted for each lap. This gives access to the mean, standard deviation, maximum and minimum for each lap. From this, it is possible to plot the raw data or the average per lap for the coefficient of friction and/or the contact resistance as a function of distance, time, or number of laps. On the fast acquisition device, it is necessary to manually synchronise the data with the tribometer data using the tribometer speed sensor voltage.

The observations of the state of wear of test samples were carried out using two complementary devices. With the use of a 3D optical profiler, Bruker Contour GT-K, it is possible to quantify the surface roughness of each sample and obtain reliable 3D visuals of the wear tracks at magnifications ranging from 2.5x to 50x. The data processing is made with the Vision64 software. In order to obtain a sharper view of the wear track on the samples, a SEM-EDX, Thermo Scientific Phenom XL G2 Desktop SEM, is used. EDX analysis of

TABLE II. Test Conditions

Designation		*Units*	*Value*
Wire		/	AuAgCu
Disc		/	AuCuX
Normal force		N	0.25
Rotating speed		RPM	500
Linear speed		m/s	0.65
Acquisition rate	Tribometer	Hz	100
	Gnostic	Hz	1 000
Current intensity		mA	100
Voltage limit		mV	500
Gain		/	10
Number of laps		/	50 000
Distance		m	3 900
Lubricant		/	None

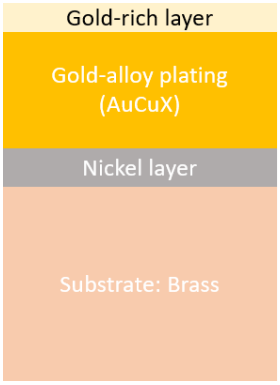

Fig. 4. Detail of the different layers composition of the disc coating (not to scale)

various spots on the surface can be performed to identify the elements present in the contact and to gain a better understanding of the material transfers in the contact. Here, an accelerating voltage of 15 keV has been chosen to better detect the presence of elements with a high atomic number such as gold. The accelerating voltage of the electron beam has a direct impact on the penetration deep into the samples. In this case, the electron-matter interaction volume is large enough to detect the major layer under the thin finish layer. There may be a risk of not accurately measuring the mass concentration of the elements at the surface, especially if the thickness of the layer or of the debris is too small.

For confidentiality reasons, one of the elements of the gold-alloy plating is designated by an X in this paper

IV. Initial State of the Contact

The initial state of the surfaces has been measured using a 3D optical profiler giving access to the 3D roughness and waviness of the samples. Fig. 5 shows the initial surface condition of the curved wire and the disc. A Vickers micro-indenter has been used to measure the hardness of the gold-alloy plating of the disc.

The 3D roughness of the wire and of the disc has been observed on three different samples from the same batch and in three different areas. The roughness measurements are averaged in Table 3. For the waviness of the discs, a larger area than that for the roughness observation has been analysed. The average waviness of the discs is 1 870 nm and it is symmetrical to the centre of the disc.

The hardness of the bulk wire is indicated by the manufacturer. The hardness of the gold alloy layer on the disc has been measured on a slice of the disc after a cross-section and a polishing with a Vickers indenter and a normal force of 49 mN. The hardness measurements are summarized in Table 3.

V. Results

Fig. 6 shows the average friction coefficient and contact resistance per lap as a function of the number of laps. The test was conducted at a linear speed of 0.65 m/s under a normal force of 0.25 N and a current intensity of 100 mA for 50 000 laps. No lubricant was used during the test. The data was collected at an acquisition rate of 100 Hz. In general, the contact resistance is stable below a value of 10 mΩ and has some variations but not exceeding 30 mΩ. These results on the contact resistance are consistent compared to the measurement done on real slip ring systems at Everaxis Aerospace & Defence. In the first 2 000 revolutions, the average friction coefficient per lap is twice around the value of 1 before decreasing and stabilising at around 0.53. From about lap 26 000 until the end of the test, the coefficient of friction increases to 0.63 and appears to be slightly more unstable than between the laps 700 and 25 000.

Fig. 7 is a zoom in of the two peaks of the friction coefficient, in which the graph A is a zoom in the first peak between lap 0 and lap 250 and the graph B is a zoom in the second peak between lap 500 and lap 2 000. The first peak between lap 0 and lap 250 is related to an increase in contact resistance. Indeed, the increase of the amplitude of the friction coefficient is synchronised with the presence of peaks in the contact resistance reaching saturation of the amplifier. The data from the high acquisition rate device (not shown here) suggests the presence of contact losses between the wire and the disc. These variations show that something happens at the contact interface during the first 250 laps. However, the peak between laps 500 and 2 000 does not show an increase in the magnitude of the friction coefficient. Here, the increase of the mean value of the friction coefficient is linked with a decrease in the mean value of the contact resistance.

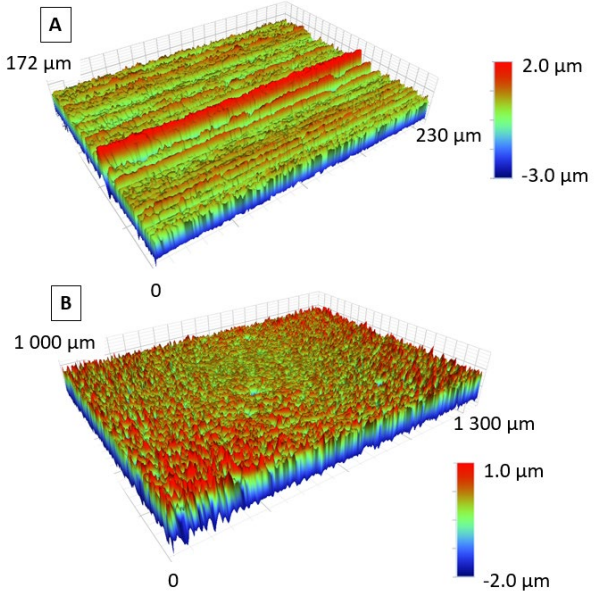

Fig. 5. Observation of the initial surfaces with a 3D optical profiler – A. wire (x27.5) 230 µm x170 µm ; B. Disc (x5) 1300 µm x1000 µm

TABLE III. Roughness & Hardness Measurements

Sample	*Sa (nm)*	*Sq (nm)*	*Sz (nm)*	*Hardness (HV)*
Wire	101	140	1 850	215
Disc	90	119	1 050	355

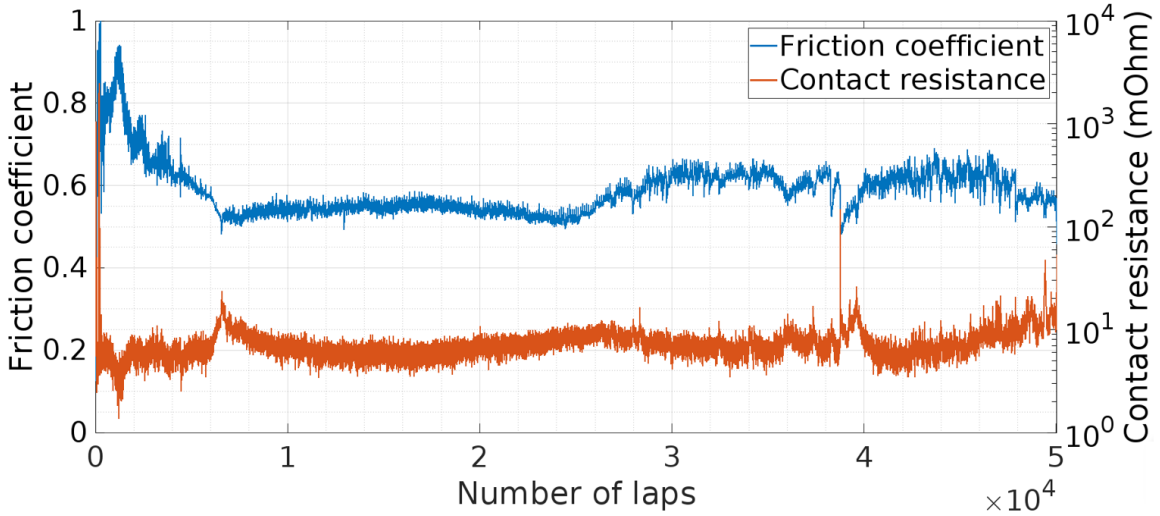

Fig. 6. Average friction coefficient (blue curve) and contact resistance (red curve) per lap as a function of the number of laps – Linear speed: 0.65 m/s; Normal load: 0.25 N; Acquisition rate: 100 Hz; Current intensity: 100 mA; Number of laps: 50 000 (1 lap = 0.078 m)

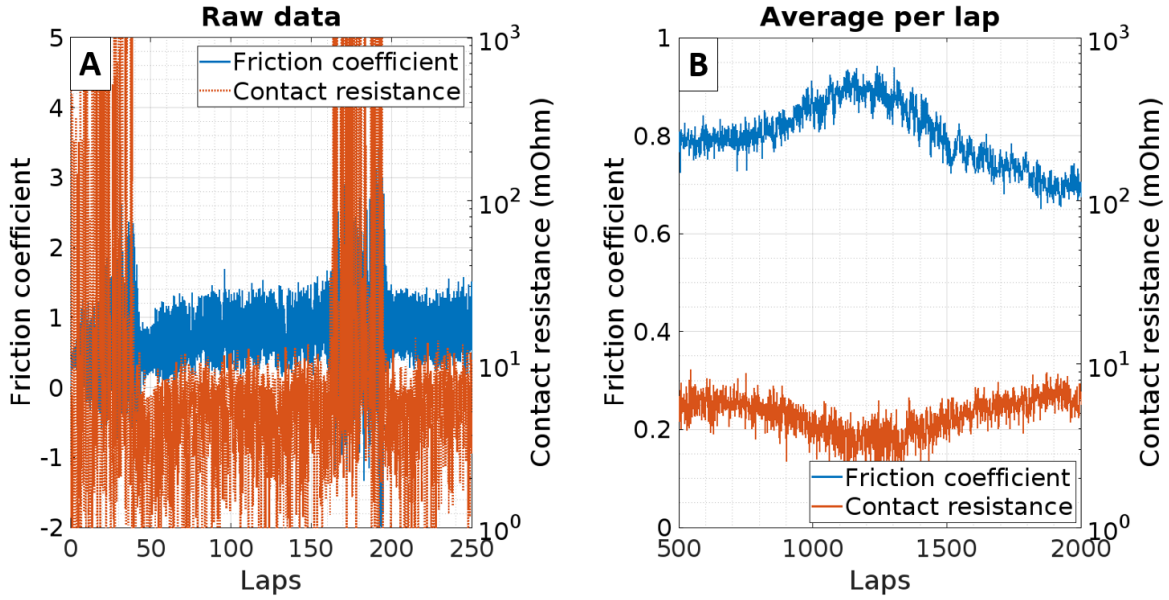

Fig. 7. Zoom in on the two peaks of the friction coefficient (blue curve) linked with the contact resistance (red curve) observed in Fig. 6 – A. Zoom in on the first 250 laps (raw data); B. Zoom in between lap 500 and 2 000 (average per lap)

Fig. 8 shows a SEM image in BSD mode of the wear track. The chemical contrast of the surfaces observed highlights the different concentrations between the worn and unworn areas. The worn area appears in dark grey while the unworn area appears in light grey. This indicates the presence of less elements with high atomic number in the wear track. The results of EDX analysis in Table 4 give access to the elements present at the surface. Compared to the unworn area, the worn area is composed of less gold and contains more copper and element X. Because, there is less gold, more copper and element X in the major layer compared to the finish layer, the EDX analysis shows that the finish layer has been worn out with the rubbing, revealing the gold-alloy layer. In the wear track, there are areas with more significant wear and with an increase in the concentration of copper and element X at the expense of gold. The observed off-track wear debris showed a weight concentration close to the gold-alloy layer.

Fig. 9 reveals the wear track on the wire; it appears brighter compared to the unworn area attesting of a surface richer in high atomic number elements. This is confirmed by the EDX analysis in Table 5 revealing that the wear track is richer in gold, copper and element X, and consequently poorer in silver compared to the unworn area. This indicates a transfer of material from the disc to the wire.

The 3D visuals in Fig. 10 obtained with the 3D optical profiler show that:

- the disc has been hollowed out with friction with an average width of 124 µm, and an average wear volume of 22 800 μm^3 for a track portion of length of 172 µm, i.e. a total wear volume of 10.4 x 10^6 μm^3 for the whole track;
- the cylindrical geometry of the wire has been flattened for a total wear volume around 3.5 x 10^6 μm^3.

VI. Discussion

Observations of the surfaces after 50 000 laps show wear of the wire, however, few or no debris from the wire (i.e. debris containing silver) are observed on the samples. The debris weight concentration is similar to the gold-alloy layer. Two shorter tests with similar test conditions, one of 1 200 laps and one of 300 laps, provided an overview of the surfaces during the first laps. It was observed on EDX analysis that silver from the wear of the wire was present in the disc track as we can observe in Fig. 11.

In the shortest test, Table 6 reveals that there were more wear debris with a silver weight concentration close to that of the initial wire than wear debris of the gold alloy plating. In this way, the event observed in the first 250 laps may be related to this. Indeed, high wear of the wire leads to the formation of conductive debris, which may cause double contact resistances in series (a contact resistance between the wire and the debris, and a contact resistance between the disc and the debris) and an increase of the risk of contact losses between the wire and the disc. This is why the magnitude of the friction coefficient and the contact resistance increase.

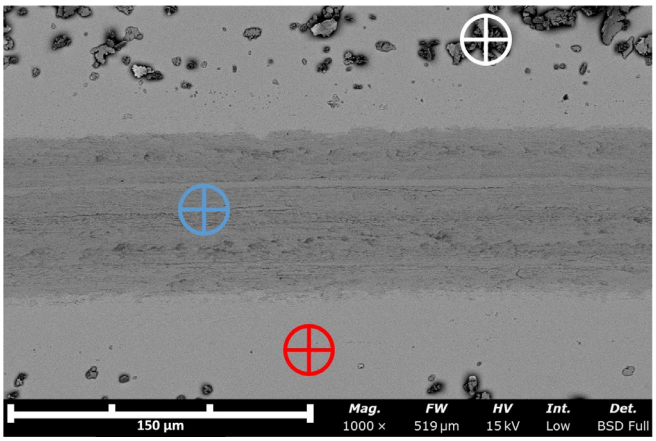

Fig. 8. Observation of the wear track of the disc after 50 000 laps with a SEM in BSD mode – x1000 – Locations of EDX analysis: light grey area corresponds to the unworn area (red cursor); dark grey area corresponds to the wear track (blue cursor); white cursor highlights the wear debris around the wear track

TABLE IV. CHEMICAL VARIATIONS (%WT) OF THE DISC WEAR TRACK (FIG. 8) COMPARED TO UNWORN AREAS USING EDX MEASUREMENT

Zone	*Au*	*Ag*	*Cu*	*X*
Red	Unworn areas			
Blue	-11%	+0%	+7%	+3%
White	-8%	+0%	+6%	+2%

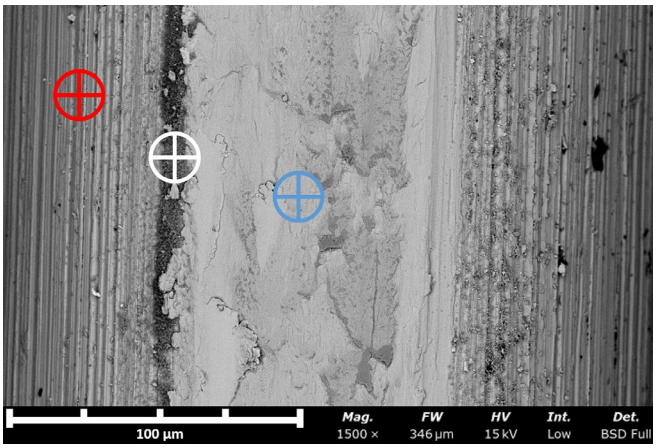

Fig. 9. Observation of the wear track of the wire after 50 000 laps with a SEM in BSD mode – x1500 – Locations of EDX analysis: dark grey area corresponds to the unworn area (red cursor); light grey area corresponds to the wear track (blue cursor); white cursor highlights the wear debris around the wear track

TABLE V. CHEMICAL VARIATIONS (%WT) OF THE WIRE WEAR TRACK (FIG. 9) COMPARED TO UNWORN AREAS USING EDX MEASUREMENT

Zone	*Au*	*Ag*	*Cu*	*X*
Red	Unworn areas			
Blue	+17%	-30%	+6%	+7%
White	-10%	-23%	+4%	+28%

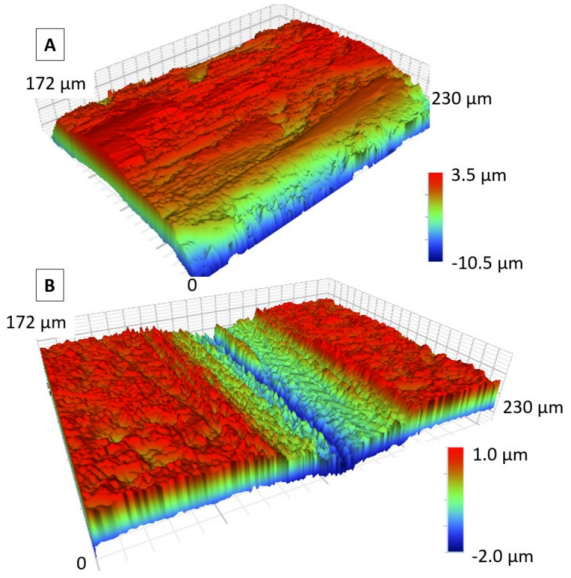

Fig. 10. Observation of the worn surfaces with a 3D optical profiler (230 µm x170 µm) – x27.5 – A. on the wire; B. on the disc

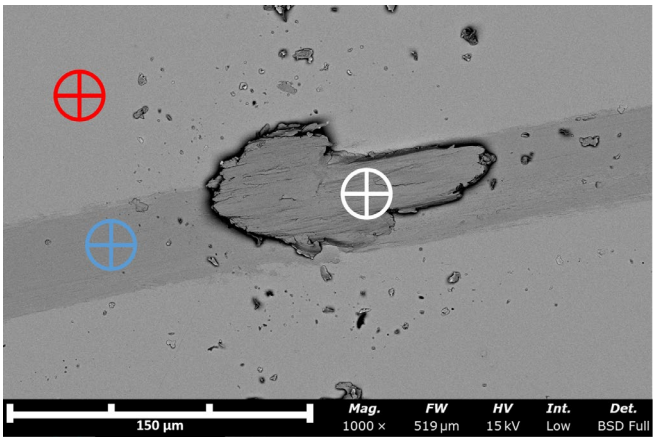

Fig. 11. Observation of the wear track of a shorter test (300 laps) of the disc with a SEM in BSD mode – x1000 – Locations of the EDX analysis: light grey area corresponds to the unworn area (red cursor); dark grey area corresponds to the wear track (blue cursor); white cursor highlights the wear debris around the wear track

TABLE VI. FOR A SHORTER TEST, CHEMICAL VARIATIONS (%WT) OF THE DISC WEAR TRACK (FIG. 11) COMPARED TO UNWORN AREAS USING EDX MEASUREMENT

Zone	*Au*	*Ag*	*Cu*	*X*
Red	Unworn areas			
Blue	-9%	+0%	+5%	+5%
White	-25%	+30%	+0%	-4%

Then, the wear of the system can be explained as follows:

- With friction, the silver-rich debris spread, split, and disperse in the wear track of the disc.
- A possible work-hardening of the wire surface leads to an increase in the wear of the disc until it becomes the majority wear.
- The formation of wear debris from the disc increases with the friction, which then transfers to the wire.

The transfer from the disc to the wire can be linked to the second peak of the friction coefficient. With the increase of contact junction between the two samples, the necessary energy to break these junctions is higher, which implies the increase of average friction force. Also, the formations of contact junctions involve a decrease of the average contact resistance. Hence, the initial friction between two different gold alloys is transformed into friction between two similar gold alloys, that of the disc. From that, the tribological system reached a steady state.

The proposed scenario of the system's wear, detailed in Fig. 12, can be summarised as follows:

1. The first rotations result in a majority of wear of the wire leading to a transfer of material from the wire to the disc. The formation of debris at the interface increases the risk of contact losses, which has a direct influence on the contact resistance and friction coefficient.
2. With friction, the debris from the wire spread and break up in the wear track of the disc leading to a work-hardening of the wire surface and then to a ploughing of the disc.

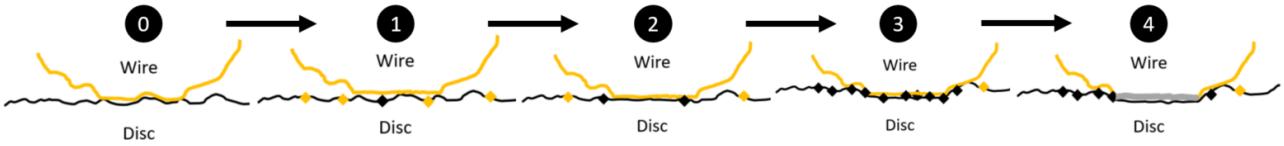

Fig. 12. Scenario on the evolution of wear in the contact interface – 0. Initial state of the contact; 1. Friction leads to a majority wear of the wire; 2. Debris from the wire spread and break up leading to a work-hardening of the wire surface and then to a ploughing of the disc; 3. Friction leads to a majority wear of the disc; 4. Formation of a hardened layer on the wire surface (grey line) thanks to the transfer of material from the disc to the wire

3. Majority wear of the wire turns into majority wear of the disc leading to the formation of debris coming from the gold alloy plating.
4. The transfer of material from the disc to the wire involves the formation of a hardened layer on the surface of the wire. The initial friction between two different gold alloys is transformed into friction between two similar alloys.

This scenario can be correlated with Antler's work [8-9] concerning the wear of metals. In the case of two metals whose rider has a lower hardness compared to the flat, he described a wear of both surfaces that transfers to the opposite surface; mostly, the wear comes from the softer surface (in the case of the present study, this is the wire). Then, with friction, the rider removes the transfer layer on the flat resulting in a work-hardening of the transfer layer on the rider. This involves a ploughing of the flat by the rider leading to the formation of debris of the flat. These debris may transfer to the rider surface leading to a friction between two identical metals. This is why the majority of wear debris is generated by the metal of the flat surface.

VII. Conclusion

In this paper, a new setup for the investigation of electrical and tribological properties of wire/ring sliding contacts has been presented. This device has been adapted from an existing tribometer initially configured for ball-on-disc contact. The ball is replaced by a curved wire mounted in a special holder, and the ring of the slip ring system is represented by a disc of the same substrate, which is coated according to an identical protocol. Furthermore, the current flow in the contact is guaranteed by a cable directly connected to the fixed wire and by brushes rubbing on the rotating disc. This offers the possibility of measuring the contact resistance with a 4-probes measurement method by doubling the connections on both elements. Thus, this device allows for simultaneous acquisition of the coefficient of friction and contact resistance during the test. In order to deal with the electrical measurement in depth, a second acquisition system allows to obtain a finer and more precise measurement of the evolution of the contact resistance. The first results show consistent measurement compared to the real slip ring systems. This new setup is intended to study the influence of various parameters on the behaviour of the gold alloy plating, such as speed, normal force, lubrication, current intensity, etc.

Furthermore, the first results have given an idea of the wear process, and a scenario has been described. In this scenario, a transition from a majority wear of the wire to a majority wear of the disc has been observed. This transition implies that the initial friction between two different gold alloys is transformed into friction between two similar alloys because of the material transfer.

This scenario needs to be further developed and confirmed with additional tests. Shorter tests and additional chemical analysis will help to better understand the running-in phase, and therefore understand the adjustment of the surfaces before reaching the steady state.

References

[1] E. Chevallier, "Définition d'indices de qualité du contact glissant métallique: Signatures électriques de l'état de surface", Thèse de doctorat. Université de Picardie Jules Verne, 2014

[2] T. Ueno, M. Aoyagi, K. Sawa, et al., "Fundamental Study of Electrical Sliding Contacts Comprising a Au-coated Slip Ring and Au Brush", In ICEC 2014; The 27th International Conference on Electrical Contacts, 2014, pp. 1-6.

[3] R. Hayes, E. Mumm, and K. Gotthelf, "Electrical noise performance of gold-on-gold slip rings", In 43th Aerospace Mechanisms Symposium, Santa Clara, California, USA, 2016, pp. 345-357.

[4] C. Holzapfel, "Test Categories for Characterization of Sliding Electrical Contacts", In 2019 IEEE Holm Conference on Electrical Contacts. IEEE, 2019, pp. 309-316.

[5] E. F. Smith, R. Lysonski, A. Klein, et al., "Screening contact materials for low speed slip ring assemblies", In Proceedings of IEEE Holm Conference on Electrical Contacts, IEEE, 1993, pp. 157-170.

[6] B. Bozzini, A. Fanigliulo, E. Lanzoni, et al., "Mechanical and tribological characterisation of electrodeposited AuCuCd", Wear, vol. 255, no 7-12, 2003, pp. 903-909

[7] M. Antler and M. H. Drozdowicz, "Wear of gold electrodeposits: Effect of substrate and of nickel underplate", Bell System Technical Journal, vol. 58, no 2, 1979, pp. 323-349.

[8] M. Antler, "Processes of metal transfer and wear", Wear, vol. 7, no 2, 1964, pp. 181-203.

[9] M. Antler, "Wear, friction, and electrical noise phenomena in severe sliding systems", ASLE TRANSACTIONS, vol. 5, no 2, 1962, pp. 297-307